

Figure S1. Cloning and purification of human ferroportin. **A**, The vector map of pPICZ-B containing the human ferroportin. **B**, SDS-PAGE of purified human ferroportin stained by Coomassie Blue. **C**, The elution profile of wild-type ferroportin on size-exclusion chromatography.

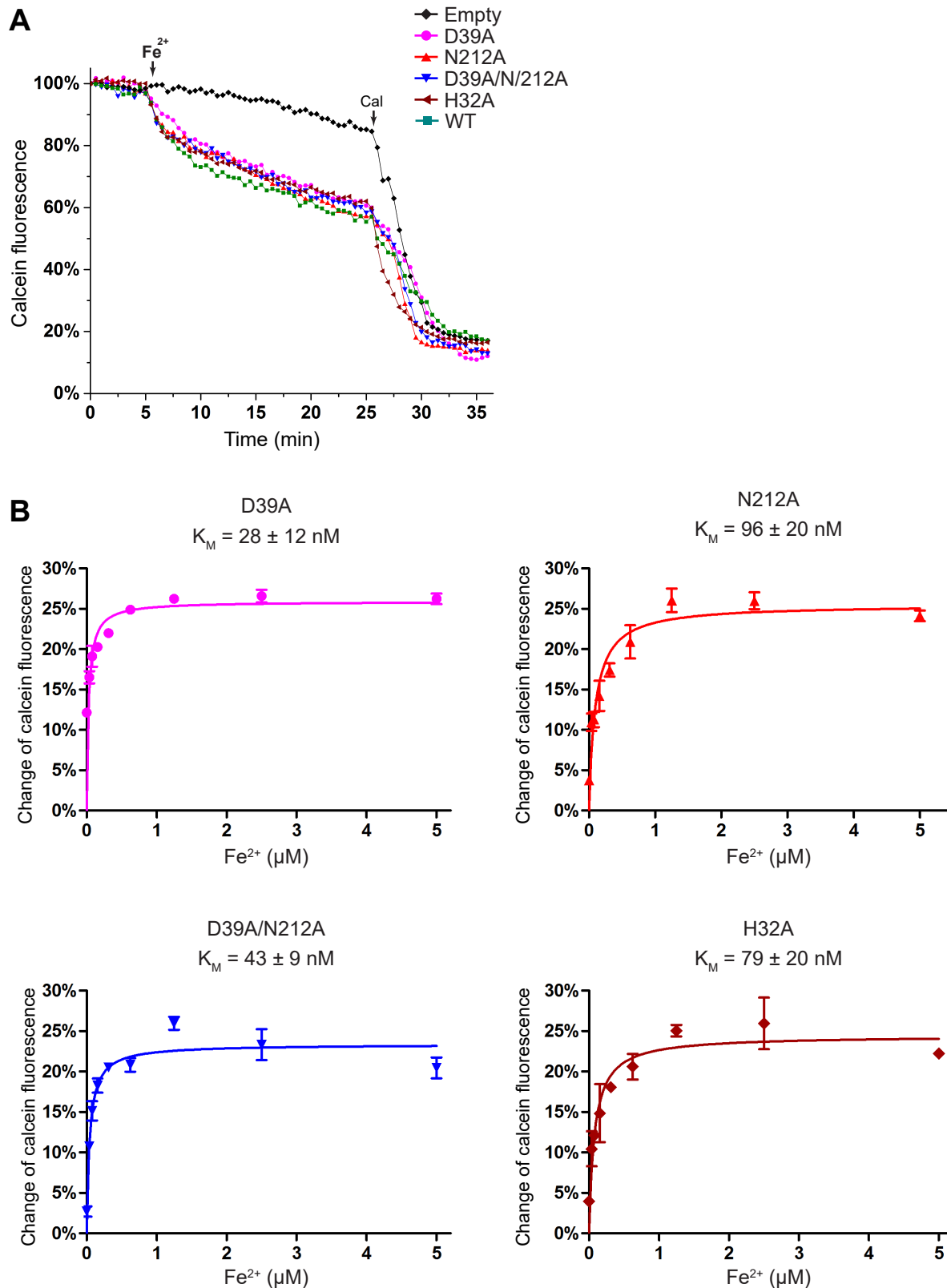


Figure S2. Iron transport activities of human ferroportin mutants. These human residues are located at the site corresponding to iron-binding site of bacterial ferroportin. **A**, Relative iron transport activities. Fe^{2+} is provided at 10 μM concentration. **B**, Michaelis-Menten curves of the human ferroportin mutants.

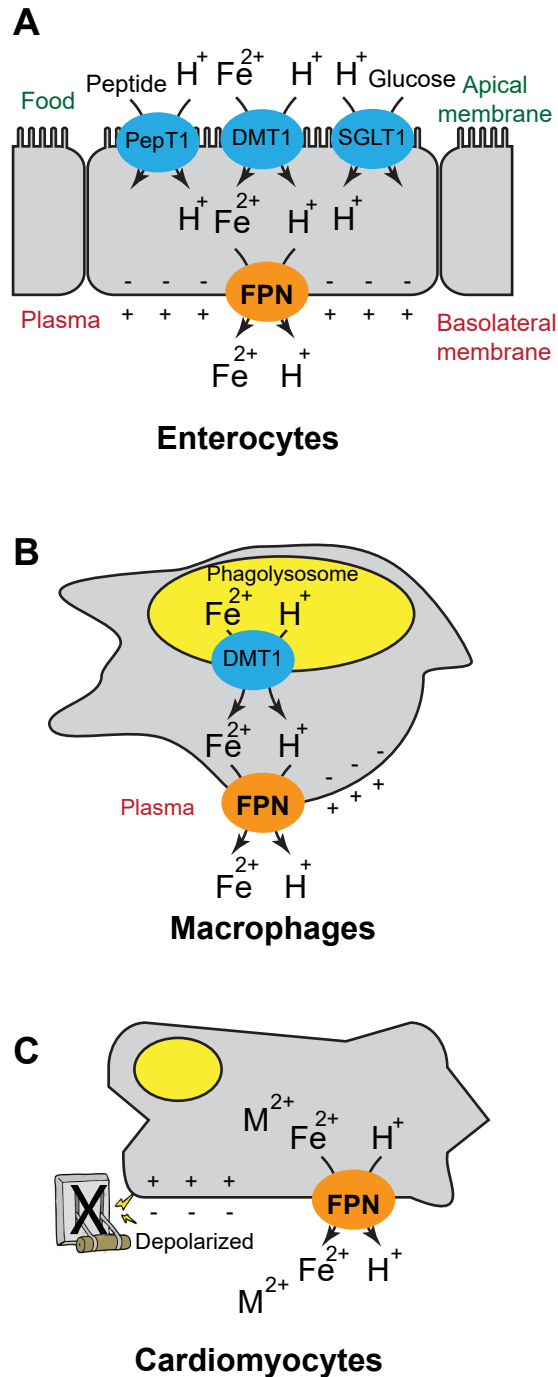


Figure S3. Hypothetical proton-facilitated iron transport under physiological conditions. A, Food absorption by duodenal enterocytes generates temporary iron and proton gradients that drive iron export via ferroportin. DMT1, PepT1 and SGLT1 represent various proton symporters located at the apical membrane of enterocytes. **B,** In macrophages, proton and iron released from phagolysosome facilitate the iron export. **C,** Depolarization in cardiomyocytes create a charge potential that facilitates iron export.